Energy Scaling and Surface Patterning of Halogen-Terminated Si(001) Surfaces

N.A. Zarkevich and D.D. Johnson [1]

Department of Materials Science & Engineering, and
Frederich Seitz Materials Research Laboratory,
University of Illinois at Urbana-Champaign, Urbana, IL 61801, USA

Abstract

We show that *steric repulsion* energies between halogen dimers on a passivated Si(001) surface scale with square of the principle quantum number (or period) n of the halogen, and arise principally from bonding with Si substrate. We exemplify the scaling from previously calculated steric interactions of F, Cl, and Br, predict the interactions for I and At, and then verify the prediction by direct density-functional calculations. From the energetics, we explain the patterning of the halogen-terminated Si(001), for a better understanding of the halogen-roughening process, and predict a crossover to a new *vacancy-line* defect for large halogens.

Key words: Surface energy; scaling; surface structure, roughness, and topology
PACS: 68.47.Fg; 68.35.-p; 81.65.Cf; 89.75.Da

Halogen roughening of silicon is an important process in manufacturing silicon-based devices. During the last few years this process is also extensively studied experimentally with scanning tunneling microscopes (STM) [1–6]. However, the science governing this process and the associated surface rearrangements are not well understood, in spite of the fact that on a Si surface halogen-halogen interactions are extremely short-ranged and dominated mostly by the nearest-neighbor *intra-* and *inter*-row repulsions (denoted by α and β, respectively). Recent measurements combined with density-functional theory (DFT) calculations have estimated *steric-repulsion* energies for light halogens on Si(001) [4]. Here we find that there is a simple scaling behavior of those energies. We show in Fig. 1 that those energies scale as n^2, where n is the period of the halogen. From this scaling, we predict a value for iodine interactions $\alpha/2$ and β, shown in Fig. 2; we verify it by DFT calculations, and show that halogen-halogen "steric" repulsion is mostly due to halogen-silicon

[1] duanej@uiuc.edu

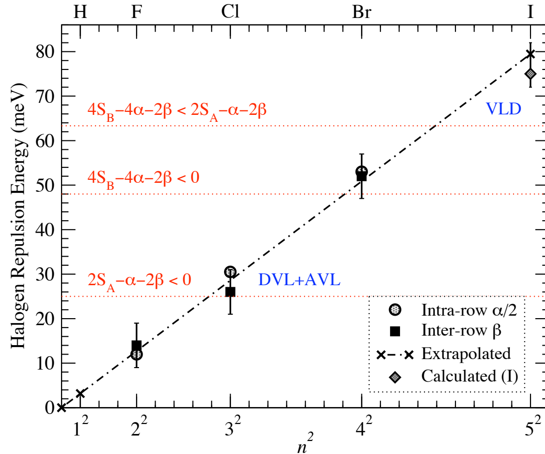

Fig. 1. Calculated intra-row $\alpha/2$ (circles) and inter-row β (squares) halogen steric-repulsion energies (in meV) vs. n^2. Values for I are from scaling (cross) and DFT (diamond). Error bar for I is shifted up by $3\,m$eV as it is relative to H-H. Patternings are determined by interactions relative to the step energies S_A and S_B, as shown in Fig. 4.

bonding, as visible from the electronic charge density isosurface in Fig 3. Relation between the scaled halogen interactions and Si(001) surface step energies not only provides a simple energy-based explanation of complex patterning produced by each halogen passivating Si(001), but also predicts new surface patterns for heavy halogens. The patterns involve atomic-vacancy lines (AVL) and dimer-vacancy lines (DVL), which are long one- and two-atom wide pits, respectively, as well as new vacancy-line defects (VLD), which are one-atom wide pits perpendicular to AVL and DVL, see Fig. 4. For large halogens (I and At), we predict a crossover to a new type of one-atom wide *vacancy-line* defects and *regrowth chains*. Our predicted VLD for iodine is now confirmed experimentally [7].

1 Scaling and DFT Verification

Halogens are reactive group VII elements, i.e., F, Cl, Br, I, and At. As with hydrogen (H), halogens may acquire a closed-shell configuration by accepting an electron from a donor atom to form an ionic-type bond, as in NaCl and KBr, or a covalent-type bond, as in HCl and HBr. On Si(001) halogens acquire the noble-gas configuration by forming a partially ionic – partially covalent bond by overlap of *s*-*p* hybrid orbitals. Hence, it is commonly believed that a steric repulsion of halogen dimers on Si(001) resembles repulsion of compressed noble gas atoms arising from the overlap of the filled electronic orbitals (indeed, known interactions of halogens on Si(001) are very short ranged). Naively, for *tethered* halogens at a fixed distance, the energy due to this overlap is roughly

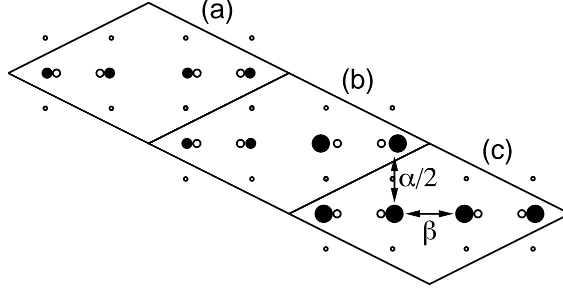

Fig. 2. Terminated Si(001) cells for (a) the H-dimers, (b) halogen and H dimers and (c) halogen-halogen dimers, where α and β interactions are labeled, with calculated relaxed atomic positions shown for I. The unit cell is denoted by the solid line in (a-c). Black large (small) circles are halogen (hydrogen) atoms above the surface. White circles (dots) are Si atoms at (below) the surface. Positions of H relative to Si in (a) and (b) are very similar, while positions of I relative to Si in (b) and (c) are very different due to I-Si bond distortion from nearest-neighbor interactions.

proportional to the radial extent of the valence shell wave-function relative to Si-Si distance, or the number of valence-shell electrons, both of which scale as n^2 for a closed shell.

In Fig. 1 we plot DFT-based $\alpha/2$ and β taken for F, Cl, and Br from Table I in [4] versus n^2. All calculated values of α and β are referenced to H-passivated Si(001), as H-H interaction is very weak ($\leq 3\,m$eV), and the number of surface bonds is maintained. Remarkably, for these terminations energies are linear in n^2 with the slope of $3.2\,m$eV, and $\beta \approx \alpha/2$ within the reported accuracy of $\pm 5\,m$eV (see also Table 1). This scaling predicts α and β for I and At.

To verify this scaling prediction, we also performed DFT calculations and found interactions for iodine. We used the Vienna *Ab initio* Simulation Package (VASP) [8–10] based on plane-wave ultra-soft pseudo-potentials [11,12], with a plane-wave energy cutoff of 349.46 eV for both H and I on Si. First, we performed DFT calculations on 4×4 cells shown in Fig. 3 in [4] with a $2\times2\times2$

Table 1
DFT and scaling based Si(001) halogen-halogen intra-row ($\alpha/2$) and inter-row (β) interactions (in meV), defect formation energies $\mathcal{A}$ and $\mathcal{B}$ (see text), calculated with S_A and S_B of 50 and $120\,m\mathrm{eV}/2a$, respectively, and resulting dominant (recessive) patterning defects, see Figs. 1 and 4 .

	n	Z	$\alpha/2$	β	$3.2n^2$	$\mathcal{A}$	$\mathcal{B}$	relations	defects
F	2	9	12	14	13	+48	+356	$0<\mathcal{A}<\mathcal{B}$	
Cl	3	17	31	26	29	−13	+184	$\mathcal{A}\lesssim 0<\mathcal{B}$	DVL→AVL
Br	4	35	53	52	51	−110	−48	$\mathcal{A}<\mathcal{B}<0$	AVL (VLD)
I	5	53	75	75	80	−200	−270	$\mathcal{B}<\mathcal{A}<0$	VLD (AVL)
At	6	85			115	−360	−670	$\mathcal{B}\ll\mathcal{A}<0$	VLD (AVL)

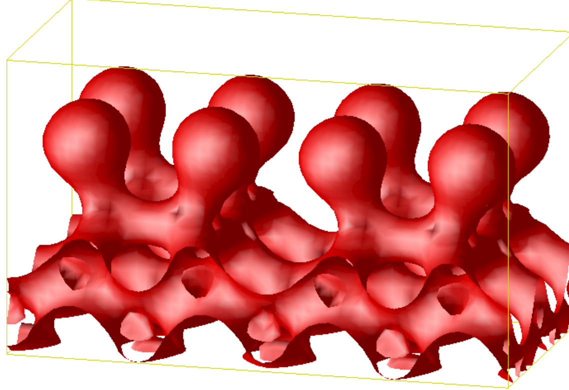

Fig. 3. Isosurface of electronic charge density at $0.3\,e^-/\text{Å}^3$ for iodine on Si(001). Positions of I and Si atoms are shown in Fig. 2c. The isosurfaces are topologically similar for $0.1 - 0.4\,e^-/\text{Å}^3$, see text.

Monkhorst-Pack [13] k-point mesh, equivalent to $8 \times 8 \times 2$ for a 1×1 cell, and we found again that $\beta \approx \alpha/2$ within the accuracy of DFT. Next, for improved accuracy, we used higher-density $4 \times 4 \times 4$ k-point mesh in smaller fixed-sized cells shown in Fig. 2. For those cells, the formation energy comprising the 'steric repulsions' is found via the following linear combination of calculated energies for various chemical decorations in Fig. 2:

$$\alpha + \beta = \frac{1}{2}(E^{(a)}_{cell} + E^{(c)}_{cell} - 2E^{(b)}_{cell})\,. \tag{1}$$

We used 7 Si layers (with the bottom two layers fixed at bulk silicon lattice constant of 5.43 Å and the lower surface terminated by H), separated by at least 15.9 Å of vacuum, for an estimated accuracy of relative energies better than ± 5 meV per formula unit. We have verified, that the energy differences would not significantly change for only 6 Si layers, but fewer (5 or less) layers are insufficient.

For all the halogens the difference between the scaling and DFT results is within the relative error of the DFT calculations. Hence, $\beta \approx \alpha/2 \approx 3.2n^2$ meV is, practically speaking, as good as direct DFT calculation. Recently our scaling- and DFT-predicted results for iodine have been confirmed by experiment [7].

2 Steric Repulsion or Bond Distortion?

An interesting question is: Do surface "steric-repulsion" energies originate from direct halogen-halogen repulsion, or rather from back-bonding of halogen to underlying Si atoms? To check, we took the cell with relaxed atomic positions of halogens on Si(001) shown in Fig. 2c, removed all the atoms except for

halogens, and passivated those four *tethered* halogens with H at the bottom. Now four halogen-silicon bonds are replaced by halogen-hydrogen bonds, and, because H atoms are much smaller than halogens, interactions are mostly direct halogen-halogen repulsions. Next, we removed all but one halogen-H molecules from this cell, and calculated the energy of a single halogen-H molecule. Difference of the energies of tethered and sparse halogen-H molecules provides an estimate of the contribution from direct halogen-halogen interaction. For iodine, this yields a direct repulsion of $(\alpha+\beta)_{steric} = 53\,m\text{eV}$, whereas the total value of $\alpha + \beta = 225\,m\text{eV}$ for I on Si(001); direct halogen-halogen interaction is *attractive* for smaller halogens.

Hence, only 24% of the energy for I is from direct halogen-halogen repulsion, while 76% is from bonding to the underlying Si and related distortion and relaxation of the Si bonds. Visualization of calculated electronic density (Fig. 3) confirms that indeed halogens are strongly bound to Si, while electronic clouds of neighbor halogens have negligible direct overlap. Comparing atomic positions in Figs. 2 (b) and (c), one can see significant distortions of relative positions of I and Si, i.e. halogen-silicon bonds, in the vicinity of other halogen dimers. In other words, the energy is dominated by distortion of halogen bonding to silicon, rather than the so-called steric repulsion.

We note that because electron charge density at the midpoint between I atoms is less then $0.1\,e^-/\text{Å}^3$, while inside Si-I bond it is greater then $0.4\,e^-/\text{Å}^3$, the charge density isosurfaces are topologically similar for $0.1 - 0.4\,e^-/\text{Å}^3$. The size of an I atom on Si(001) in Fig. 3 is between iodine atomic (1.3 Å) and ionic (2.2 Å) radii, due to partially ionic–partially covalent nature of the Si-I bond. [2]

3 Surface Patterning

3.1 Energetics of Passivation and Si Steps

Most features of patterning produced by halogen roughening are determined by cross-over energetics and can be explained from halogen-halogen intra-row α and inter-row β interactions and silicon surface step energies, see Fig. 4. The measured S_A and S_B step energies on Si(001), which inherently reflect full relaxations, are reported from Table 2 in [14], with $S_A = 52 - 64$ and $S_B = 120 - 140\,m\text{eV}$ per $2a$, where $a = 3.84$ Å is the Si(001) surface lattice constant.

[2] The average density for I accepting 1 electron (e^-), for a total of 15 valence electrons, is $0.3\,e^-/\text{Å}^3$.

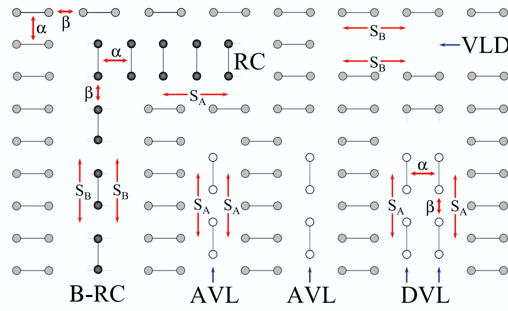

Fig. 4. Line defects on Si(001) and their energetics. White, grey, and dark circles represent passivating atoms (dimers) in the lower, main, and upper terraces, respectively. α and β are intra- and inter- row interactions between dimers. DVL, AVL, and RC are previously known surface line defects bounded by S_A steps, energetically favorable if $\mathcal{A} \equiv 2S_A - \alpha - 2\beta < 0$. VLD and B-RC are new types of line defects bounded by S_B steps, which become possible if $\mathcal{B} \equiv 4S_B - 4\alpha - 2\beta < 0$, and stable if $\mathcal{B} < \mathcal{A}$. The energy costs are outlined in text.

If roughening happens, atoms are removed from pits and added to islands, and surface patterns are created by line defects oriented either along S_A or S_B steps. Formation of defects bounded by S_A steps is detailed in [4]: primary roughening results in DVL formation; next, a DVL splits into two AVL during secondary roughening. Here we also consider a new type of roughening, that results in VLD oriented along S_B steps, revealing a crossover to this new type of defects.

Let us look in Fig. 4, compare roughening energies of DVL and VLD, and make a prediction as to which patterning is more energetically favorable. Consider a DVL created on a pristine surface: for each two Si dimers removed, two S_A steps are created, and 2α and 4β interactions are eliminated on the main terrace, while 1α and 2β interactions are introduced on the lower terrace. Hence, a DVL energy is $\mathcal{A} \equiv 2S_A - \alpha - 2\beta$. Now considering a VLD created on a pristine surface: for each two Si dimers removed, four new S_B steps are created, and 4α and 2β interactions are eliminated on the main terrace, while no new interactions on the lower terrace appear. Hence, a VLD energy is $\mathcal{B} \equiv 4S_B - 4\alpha - 2\beta$. We will detail the patterning in section 3.3. Obviously, a VLD will form instead of DVL if $\mathcal{B} < \mathcal{A}$. In other words, if $\mathcal{B} < \mathcal{A} < 0$, then new line defects directed along S_B steps will make Si(001) surface pattens.

3.2 S_B Steps and Atom Conservation

Notably, formation of S_B steps includes rebonding and thus does not preserve the number of passivating atoms; the energy of this rebonding is already included in the experimental value. Also, a fully-covered silicon surface may

roughen only by etching, because free surface sites are needed for other types of surface kinetics (indeed, steric roughening of a fully-covered surface is not observed in experiment [7]). If one consider a halogen-covered Si sample at a finite temperature in vacuum, there is also a loss of halogen atoms from surface over time. As a result of this loss, new surface vacancies are created; those vacancies make possible atomic rearrangements on the surface leading to roughening, and, in particular, allow formation of new S_B steps.

Previously it was shown how to preserve the number of atoms in energy calculations by preserving the number of S_B steps: for example, in Fig. 7a in [5] this was achieved by forming a 1-dimer island. Unfortunately, that reasoning can not tell if there are any S_B steps, or how and why initial roughening (including or not one-dimer vacancies) occurs. Comparing Figs. 5a and 7a in [5], one can conclude that, if there are one-dimer vacancies on the surface, then growth of VLD (see our Fig. 4) is energetically favorable if $\beta > S_A$, as for iodine and heavier halogens, while for lighter halogens with $\beta < S_A$ DVL should grow. Surprisingly, this simple conclusion is correct for Cl, Br, and I, and fails for F, which is highly reactive and roughens Si surface by etching. However, other STM observations [7] demonstrated that neither the number of S_B steps nor the number of passivating atoms remains constant during experiment.

Below we allow the possibility of creating new S_B steps, and assume, that the number of passivating atoms might change, but the experimentally assessed energy of S_B steps takes this non-conservation into account.

3.3 Energetically Favorable Patterns

Because second-neighbor interactions are negligible [4], the surface patterns are mostly determined by the interplay between the inter-row and intra-row nearest-neighbor repulsions $\beta \approx \alpha/2$ and the relative energies of the surface steps $S_A \approx S_B/2$, which are positive. Thus, it is clear that $0 < S_A < S_B$ and $0 < \beta < \alpha$ for all halogens. Considering Si(001) vacancy lines (pits), as represented in Fig. 4, we can now predict the dominance (and crossover) of VLD, DVL and AVL, which define preferred patterning orientations, based on the relative energies of A and B steps and intra-row α and inter-row β interactions, namely, $\mathcal{A} \equiv 2S_A - \alpha - 2\beta$ and $\mathcal{B} \equiv 4S_B - 4\alpha - 2\beta$ (in meV per two dimers). Here $2\mathcal{A}$ is energy to create DVL with RC; $\mathcal{A}$ is energy to split DVL into two AVL. The DVL, AVL, and RC are bounded by A steps; the DVL result from primary roughening, and the AVL result from secondary roughening by light halogens, as already detailed in [4]. $\mathcal{B}$ is energy associated with a new vacancy line defect. The VLD is bounded by B steps and is perpendicular to both DVL and AVL. Comparing energies $\mathcal{A}$ and $\mathcal{B}$, we can now predict dominant surface defects and preferable patterning orientation

for each halogen.

A synopsis of the overall expectation on a pristine surface is given in Table 1 and Fig. 1. If $\mathcal{A} < 0$, then formation of a DVL followed by its splitting into two AVL is energetically favorable; in addition, if $\mathcal{B} < 0$, then formation of VLD is energetically favorable on a flat Si(001) surface. If both are negative such that $\mathcal{A} < \mathcal{B} < 0$, then AVL dominate; otherwise, VLD dominate if $\mathcal{B} < \mathcal{A} < 0$. The possibility of DVL and AVL among pits implies possibility of 2-atom-wide dimer regrowth chains (RC) among islands; if VLD dominate, then 1-atom-wide B-type regrowth chains (B-RC), bounded by S_B steps, are possible. Directions of all these narrow defects are related: DVL $\parallel$ AVL $\perp$ VLD $\parallel$ RC $\perp$ B-RC, see Fig. 4. We note that VLD and B-RC are new types of surface defects, and a VLD is now observed experimentally [7].

If β and α are significantly smaller than the step energies S_A and S_B (i.e., both $\mathcal{A} > 0$ and $\mathcal{B} > 0$), as is for F, then the sterically-driven roughening is not favored, although other roughening mechanisms (*e.g.*, chemical etching) are possible. Indeed, fluorine is highly reactive and does not stay in the assumed termination [15], hence, these energetics are less useful.

For chlorine, $\mathcal{A} = -13$ meV, thus, it is weakly unstable and sterically-driven roughening occurs: most islands and pits are at least two atoms (one dimer) wide, and, due to small energetics, which is on the order of 150 K, DVL$\rightarrow$AVL transition is slow, as is observed [16]. Sterically-driven patterning is energetically more favorable for heavier halogens, as can be seen in Fig. 1

For bromine, where $\beta \approx S_A$, it is very energetically favorable for DVL to form and split into two AVL with $\mathcal{A} = -110$ meV. Also, because $\mathcal{B} = -48$ meV, formation of VLD on a pristine surface is possible, although AVL are significantly more energetically favorable and thus dominant.

For both Cl and Br, directions of narrow pits and islands are perpendicular and determined by the S_A step edges bounding them. Although steric repulsion does not explain roughening due to chemical etching by F or by halogens at small surface coverage ($< 1/2$), it accounts for periodic pattern of AVL created by partial Br coverage greater than 1/2.

Finally, for iodine, where $\beta \approx 75\,m$eV, $\mathcal{A} = -200$ and $\mathcal{B} = -270\,m$eV, see Table 1 and Fig. 1. Because $\mathcal{B} < \mathcal{A} < 0$, new surface defects (VLD and B-RC) bounded by B steps become more energetically stable and thus dominant. However, the AVL and RC directions are still governed by A steps. Because A and B steps are perpendicular, we have AVL $\perp$ VLD $\parallel$ RC $\perp$ BRC, see Fig. 4. The steric-repulsion energy and patterning for astatine may be similarly estimated.

4 Summary

Steric-repulsion energies associated with halogen-passivated Si(001) scale as n^2, where n is the period of the halogen. We verified the scaling-predicted results for iodine by a DFT calculation, and showed that halogen-halogen interactions are not direct, but mostly due to halogen-silicon bonding. From the scaling we predicted the change in surface patterning versus halogen termination, including new defects (one-atom-wide *vacancy-lines* and *B-type regrowth chains* oriented along S_B steps) and a crossover in orientation of defects, recently observed experimentally with iodine [7]. The scaling energetics may be used within Monte Carlo simulations to explore temperature-dependent effects on patterning. As halogen roughening of Si(001) surfaces is an important technological process in manufacturing silicon-based devices, we hope to have provided better understanding on the science governing this process and the associated surface rearrangements, as well as a simple means to predict their occurrence.

Acknowledgments

We thank L.-L. Wang, J.H. Weaver and G.J. Xu for helpful suggestions and comments. Our support came from the U.S. Department of Energy, Division of Materials Sciences under Award DEFG02-91ER45439 and Catalysis under Award DEFG02-03ER46026, both through the Frederick Seitz Materials Research Laboratory at the University of Illinois at Urbana-Champaign. Computational resources provided by the Materials Computation Center under National Science Foundation grant DMR-0325939, and an equipment grant from Intel Corporation.

References

[1] J.J. Boland and J.H. Weaver, Physics Today 51 (1998) 34–40.

[2] M. Chander, D.A. Goetsch, C.M. Aldao, and J.H. Weaver, Phys. Rev. Lett. 74 (1995) 2014–2017.

[3] K. Nakayama and J.H. Weaver, Phys. Rev. Lett. 82 (1999) 568–571.

[4] C.F. Herrmann, D. Chen, and J.J. Boland, Phys. Rev. Letters 89 (9) (2002) 096102.

[5] D. Chen and J.J. Boland, Phys. Rev. B 67 (2003) 195328.

[6] G.J. Xu, S.V. Khare, K.S. Nakayama, C.M. Aldao, and J.H. Weaver, Phys. Rev. B 68 (2003) 235318.

[7] G.J. Xu, N.A. Zarkevich, Abhishek Agrawal, A.W. Signor, D.D. Johnson, and J.H. Weaver, Phys. Rev. B 71 (2005) 115332.

[8] G. Kresse, J. Hafner, Phys. Rev. B 47 (1993) RC558.

[9] G. Kresse, J. Furthmüller, Comp. Mat. Sci. 6 (1996) 15.

[10] G. Kresse, J. Furthmüller, Phys. Rev. B 54 (1996) 11169.

[11] D. Vanderbilt, Phys. Rev. B 41 (1990) 7892.

[12] G. Kresse, J. Hafner, J. Phys. C: Condens. Matter 6 (1994) 8245.

[13] H.J. Monkhorst and J.D. Pack, Phys. Rev. B 13 (1976) 5188.

[14] H.J.W. Zandvliet, Rev. Mod. Phys. 72 (2) (2000) 593–602.

[15] K.S. Nakayama and J.H. Weaver, Phys. Rev. Lett. 83 (1999) 3210–3213.

[16] G.J.Xu, E.Graugnard, V.Petrova, Koji S. Nakayarna, and J.H.Weaver, Phys. Rev. B 67 (2003) 125320.